Formation of a Dense Branching Morphology in Interfacial Growth

E. Ben-Jacob,[1,2] G. Deutscher,[2] P. Garik,[1,2] Nigel D. Goldenfeld,[3] and Y. Lareah[2]

[1]*Department of Physics, Randall Laboratory, University of Michigan, Ann Arbor, Michigan 48109*

[2]*Department of Condensed Matter Physics, School of Physics and Astronomy, Tel Aviv University, 69978 Tel Aviv, Israel*

[3]*Loomis Laboratory of Physics and Materials Research Laboratory, University of Illinois at Urbana-Champaign, Urbana, Illinois 61801*

(Received 1 April 1986)

We present experimental evidence of a distinct dense branching morphology as a fundamental pattern for diffusion-controlled interfacial growth. The dense branching morphology is characterized by its circular envelope modulated by leading branch tips. The development of this pattern in two dimensions is studied in a Hele-Shaw cell and in amorphous annealing. We find agreement between the Hele-Shaw experiment and a linear stability analysis including a kinetic term.

PACS numbers: 61.50.Cj, 05.70.Ln, 68.70.+w, 81.30.Fb

The patterns observed in nonequilibrium systems have been the objects of intense scrutiny over the past few years. It is now recognized that variation of the control parameters in diffusion-controlled systems gives rise to a number of distinct morphologies. Simple experiments of fluid flow in modified Hele-Shaw cells[1] and two-dimensional electrodeposition[2,3] have produced the first morphology diagrams displaying the regimes of faceted, tip-splitting and dendritic growth as functions of the control parameters. Moreover, these morphologies are observed on length scales ranging from the submicron to centimeters. For example, the dendritic morphology is observed from the macroscopic scale (~ 10 cm) in anisotropic Hele-Shaw experiments down to the mesoscopic scale (submicron) in electrochemical deposition.

In the absence of sufficient anisotropy to produce dendritic growth, repeated tip splittings dominate the interfacial dynamics in diffusion-controlled growth.[4,5] The purpose of this paper is to show that tip splitting gives rise to a new distinct morphology. This is a dense branching morphology (DBM) characterized by a stable circular envelope modulated by leading branch tips. We have observed this morphology on the centimeter scale in a radial Hele-Shaw cell, and on the micron scale in the annealing of amorphous $Al_{0.4}Ge_{0.6}$. Additional support for this morphology is provided by its observation in electrochemical-deposition experiments[2,3] and lipid crystallization.[6] As a first analytic attempt to understand our observations, we have performed a linear stability analysis for the Hele-Shaw interface including a kinetic term as part of the interfacial boundary condition. The analysis results in a fastest-growing mode which strongly suggests that the DBM should be characterized by the number of branches as function of radius. Although a full understanding of the dense branching morphology requires nonlinear analysis, the linear analysis presented below is consistent with our experiments and with earlier experiments in electrochemical deposition. Moreover, an extension of this linear stability analysis to three dimensions suggests that the spherulitic structure observed in melt-grown polymer crystals[7] and in vitreous igneous rocks[8] is the DBM.

The emergence of a dense branching morphology is in contrast to a previous hypothesis[1,9] that tip-splitting dynamics give rise to a fractal morphology like that obtained in simulations of diffusion-limited aggregation (DLA).[10] This hypothesis has until now been found consistent with simulations of DLA with surface tension,[11,12] a numerical solution to the Hele-Shaw equations,[9] a deterministic algorithm for on-lattice aggregation,[13] an experiment in a small radial Hele-Shaw cell,[1] a Hele-Shaw experiment employing non-Newtonian fluids,[14] and electrochemical-deposition experiments.[15,16] Our stability analysis indicates that the initial branching rate of the DBM is similar to that of the DLA morphology. However, the dense branching morphology is not fractal: The lacunae do not scale with the size of the object. On the basis of our analysis we now view the DLA morphology as the limit of the DBM for vanishing effective surface tension as defined below.

Our Hele-Shaw cell experiment was performed with use of Paterson's radial geometry.[17] The plates were Plexiglas with the upper one $\frac{3}{4}$ in. thick and 23 in. in diameter; the lower plate was a square sheet 1 in. thick. The two plates were flat to a tolerance of approximately 0.005 in. The range of spacings between the plates used was 0.4–0.8 mm. Our viscous fluid was glycerol. The working temperature was $T = 22 \pm 0.2$ °C with a corresponding viscosity of the glycerol of 1200 cP. Oxygen gas was injected into the center of the cell under pressure. The variation of pressure during the experiment was ≈ 2 mm of Hg. We repeated the experiment for pressures ranging from 50 to 150 mm of Hg. In order to avoid lifting of the plates (the applied force was up to ≈ 2000 N) six 6-in. C clamps were applied symmetrically around the boundary, and metal bars were clamped diametrically

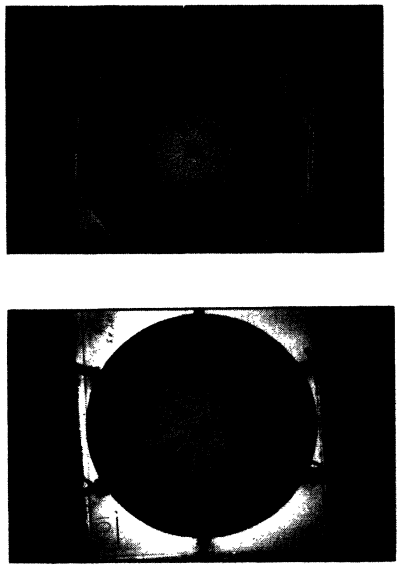

FIG. 1. The dense branching morphology generated in the Hele-Shaw cell described in the text. (a) Air into glycerol at applied pressure of 100 mm of Hg and spacing of ≈ 0.5 mm. (b) Water into glycerol at flow rate of 50 ml/min and spacing of ≈ 0.5 mm.

across the cell above and below each other. The same basic morphology was observed in all cases with the minimum length scale varying as a function of the spacing.[18] An example of the pattern is shown in Fig. 1(a). The stable circular envelope observed developed repeatedly even under less than perfect conditions. We repeated the Hele-Shaw experiment with miscible fluids. With use of the same cell, water was injected into the glycerol. The same morphology developed. The experiment was performed at constant flow rates of the water ranging from 25 to 250 ml/min. Because of the miscibility of the two fluids, there is no equilibrium surface tension but a dynamic interfacial tension resulting from a competition of the time scales for the advance of the interface and the diffusion rates between the two fluids. The effect of this reduced surface tension, as seen in a comparison of Figs. 1(a) and 1(b), is to produce a more open structure. The noisy bumps on the main stalks are also observed to be more pronounced than in the air-into-glycerol pattern.

As a first step to understand the dense branching morphology, we have done a linear stability analysis for the Hele-Shaw cell by analogy to a Mullins-Sekerka analysis.[19] The new element in our analysis is the inclusion of a kinetic term in the interfacial boundary condition. Such a kinetic term has proven important in the explanation of dendritic growth in solidification,[4,5] and gives rise to dendritic growth distinct from that which arises from surface tension alone in anisotropic Hele-Shaw experiments.[20] The Gibbs-Thomson relation, including a kinetic term proportional to the normal velocity at the surface, v_n, is $p_s = p_g - d_0\kappa - \beta v_n^{\gamma}$, where p_s is the pressure in the fluid at the interface, p_g is the applied air pressure, d_0 is twice the interfacial surface tension, κ is the curvature of the interface, the pressure field $p(r,\theta)$ satisfies Laplace's equation as described in Ref. 1, and $\gamma = 1.0$ is assumed here for a Newtonian fluid. We consider a perturbed envelope given by $R_s(\theta) = R + \delta_m \cos(m\theta)$ with $\delta \ll R$. The time development of the perturbation δ_m is given by

$$\alpha_m(x) = \frac{\dot{\delta}_m/\delta_m}{\dot{R}/R} = -1 + \frac{m}{m\bar{\beta} + x[(1-x^{2m})/(1+x^{2m})]}\left[x + \bar{\beta} - \frac{(m^2-1)[x\ln(1/x)+\bar{\beta}]}{\xi x - 1}\right], \tag{1}$$

$$\xi = (p_g - p_0)/(d_0/R_0), \quad \bar{\beta} = \beta b^2/(12\eta R_0), \quad x = R/R_0,$$

where p_0 is the pressure at the radius R_0 (the radius of the cell), b is the plate spacing, and η is the viscosity. A study of (1) shows that there exists a fastest-growing mode, $m^*(x)$, which maximizes α_m. We hypothesize that the observed number of major branches, m_b, can be approximated by $m^*(x)$. m_b can be measured by taking the power spectrum of the interface. A careful study of the power spectrum of the interface has been performed by Rauseo, Barnes, and Maher.[21] In our Hele-Shaw experiment we find additional peaks which correspond to slow modulation of the interface and to the width of individual fingers. Our hypothesis is motivated by the result of the Rayleigh-Bénard and Couette-Taylor experiments where the selected wavelength, determined by nonlinear effects, is close to that of the fastest mode in the vicinity of the critical Reynolds number. Figure 2 shows the agreement of the fastest-growing-mode hypothesis with results of our Hele-Shaw experiment. The value of m^* is determined by the interplay between the stabilizing effect of both the effective surface tension (i.e., ξ^{-1}) and kinetic terms, and the destabilizing effect of the diffusion field. In this context, the much greater branching observed in electrochemical deposition[2,3] corresponds to a substantially smaller effective surface tension.

By use of Eq. (1) the parameter regimes in which the branching structure of the DBM has previously been analyzed as a fractal object can be studied. For a fractal object the branching rate behaves like $\sim x^{D-1}$, where D is the fractal dimension. Although the DBM is not fractal, we can use $m^*(x)$ to compute an effective branching exponent: $\nu(x) = d\ln m^*/d\ln x$. For

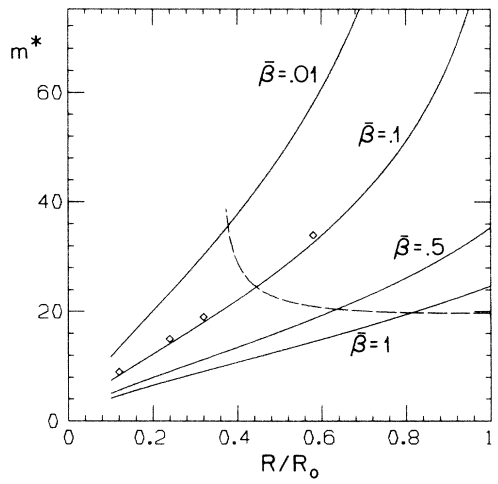

FIG. 2. Plot of the fastest-growing mode (solid line) as a function of x and varying $\bar{\beta}$. The broken line is a plot of m^* as a function of x_c. The parameter $\xi = 1.6 \times 10^4$, as determined by use of $d_0 = 126$ dyn/cm, $b = 0.4$ mm, $R_0 = 23$ in., and $p_g - p_0 = 50$ mm Hg. The diamond-shaped points designate the number of experimentally counted main branches m_b for air into glycerol in an experiment with the above parameters. We estimate the value of $\bar{\beta}$ in this experiment to be ~ 0.1 using an heuristic argument. In the direction normal to the plates the viscous-fluid front's profile can be approximated by a parabola (Ref. 22). The fluid "left behind" the advancing parabolic tip is a narrow wetting layer. In order for this layer to advance as well, there must be an additional pressure drop on the fluid side of the interface. As an order of magnitude, we estimate the width of this wetting layer as roughly 0.1 of the plate spacing. It follows that if the wetting layer is to move with the tip then $\bar{\beta} \sim 0.1$.

$x \approx 0.1$ [the definition of $\nu(x)$ is meaningless for smaller x], ν is approximately 0.7 with a weak dependence on the parameters. In this range the DBM may display the mass distribution of the DLA morphology in both theoretical and experimental studies. However, $\nu(x)$ increases with x and equals 1.0 for a value x_c. Regular branching in two dimensions is not possible for $\nu > 1.0$. At this crossover point we can speculate on the existence of a change in structure of the morphology. This may be observable as a change in the power spectrum of the interface. Predicting the nature of such a change is beyond the scope of linear stability analysis and requires a nonlinear study. However, the point x_c can be calculated. Doing so, we find that x_c depends very weakly on ξ and for $0.05 \leq \beta \leq 0.5$, x_c ranges from 0.4 to 0.8. Moreover, in the limit of vanishing effective surface tension ($d_0/R_0 \rightarrow 0$), $\xi \rightarrow \infty$ and $\alpha_m \sim m - 1$; in this limit m^* diverges, which according to our interpretation corresponds to the DLA limit in agreement with an earlier conjecture.[10]

We now discuss an amorphous-annealing experiment which also gives rise to the dense branching on a micron scale, as shown in Fig. 3. Amorphous $Al_{0.4}Ge_{0.6}$ alloy films, 600 Å thick, were prepared by simultaneous evaporation of Ge and Al by electron guns in a vacuum of 2×10^{-6} Torr onto a microscope slide covered with soluble material and held at room

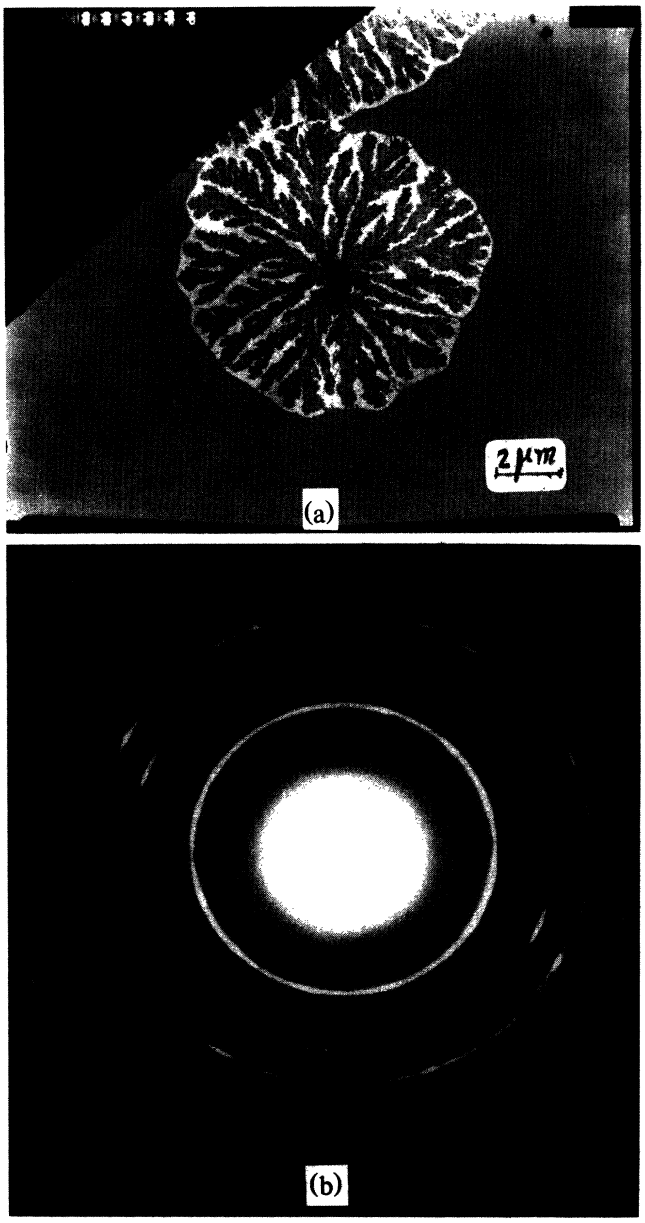

FIG. 3. (a) The DBM generated in the annealing of amorphous $Al_{0.4}Ge_{0.6}$. The dark structure is polycrystalline Ge. The light background is the crystalline Al matrix described in the text. The surrounding dark background is amorphous $Al_{0.4}Ge_{0.6}$. (b) Electron diffraction pattern from a dense branching morphology like that in (a). The bright arc spots are the (111) planes of Al. The rings are due to the diamond structure of polycrystalline Ge.

temperature. The film was then heated in a transmission-electron microscope. At a temperature of 230 °C the dense branching structure was observed to form at many sites. As inferred from Fig. 3(b), its microscopic structure is that of polycrystalline Ge. This growth results in an Al-rich region surrounding the Ge. As determined by electron-diffraction studies, Fig. 3(b), this Al envelope is a nearly perfect crystal. Although the governing microscopic physics is still under investigation, we believe that the rate-limiting step for the growth of the branching structure is the diffusion of Ge from the amorphous matrix through the Al-enriched region. To date we have not observed dendritic growth during this annealing process in $Al_{0.4}Ge_{0.6}$. By contrast, growth of dendrites, as well as dense branching, has been observed in the annealing of amorphous In_2O_3 films.[23] We speculate that the mismatch of crystal structures between Al (fcc) and Ge (diamond structure) suppresses the effective anisotropy necessary for the formation of dendrites. Moreover, the formation of polycrystalline Ge during amorphous annealing, as opposed to the crystalline form of Al, is similar to the change in crystal structure of Zn during dense branching growth in electrodeposition.[3] In both cases, the change in macroscopic morphology is coincident with a change in microscopic structure.

Finally, linear stability analysis in three dimensions also results in a fastest-growing mode. This leads us to suggest that the DBM can exist in three dimensions.[24] Both vitreous igneous rocks and melt-grown polymer crystals exhibit spherulites.[7] Usually attributed, not to thermal diffusion, but to segregation of polydisperse chains, the growth of spherulites nevertheless occurs by the same type of diffusion processes as those occurring in dendritic growth.[8,24] Thus, we speculate that in these systems, the anisotropy is too weak for dendritic growth to occur, and the DBM is found instead. This is consistent with the observations of noncrystallographic branching in these systems.

To conclude, in diffusion-controlled systems with weak effective anisotropy a new and distinct morphology evolves which appears to be the complementary morphology to dendritic growth. Above we have reported observation of this dense branching morphology in Hele-Shaw and amorphous-annealing experiments. We further find that earlier electrochemical-deposition[2,3] and lipid-crystallization experiments[6] also resulted in dense branching structures. Analysis of the Hele-Shaw experiment strongly suggests that the best way to characterize this morphology is by m_b, the number of branches at a given radius; that the fastest-growing mode found by a linear stability analysis is a good approximation to m_b; and that kinetic effects must be considered in determining the branching rate. This analysis also suggests why the mass distribution of the DBM may be mistaken for that of the DLA morphology under certain experimental conditions.

We thank V. Steinberg for sharing with us his results, D. Grier, D. Kessler, and L. M. Sander for useful discussions. E.B.-J. is a Bat-Sheva Fellow and also gratefully acknowledges receipt of the Rackham Award. This research was supported in part by a grant from the Israel Council for Basic Research, and by National Science Foundation Grant No. DMR84-05355.

[1]E. Ben-Jacob, R. Godbey, N. D. Goldenfeld, J. Koplik, H. Levine, T. Mueller, and L. M. Sander, Phys. Rev. Lett. **55**, 1315 (1985).

[2]Y. Sawada, A. Dougherty, and J. P. Gollub, Phys. Rev. Lett. **56**, 1260 (1986).

[3]D. Grier, E. Ben-Jacob, R. Clarke, and L. M. Sander, Phys. Rev. Lett. **56**, 1264 (1986).

[4]E. Ben-Jacob, N. D. Goldenfeld, J. S. Langer, and G. Schön, Phys. Rev. Lett. **51**, 1930 (1983), and Phys. Rev. A **29**, 330 (1984); E. Ben-Jacob, N. D. Goldenfeld, B. G. Kotliar, and J. S. Langer, Phys. Rev. Lett. **53**, 2110 (1984).

[5]R. Brower, D. Kessler, J. Koplik, and H. Levine, Phys. Rev. Lett. **51**, 1111 (1983), and Phys. Rev. A **29**, 1335 (1984); D. Kessler, J. Koplik, and H. Levine, Phys. Rev. A **30**, 3161 (1984).

[6]A. Miller, W. Knoll, and H. Möhwald, Phys. Rev. Lett. **56**, 2633 (1986).

[7]B. Wunderlich, *Macromolecular Physics* (Academic Press, New York, 1973), Vol. 1, pp. 295–325; P. H. Geil, *Polymer Single Crystals* (Wiley Interscience, New York, 1963).

[8]H. D. Keith and F. J. Padden, J. Appl. Phys. **34**, 2409 (1963). For a recent review see D. C. Bassett, Crit. Rev. Solid State Mater. Sci. **12**, 97 (1986).

[9]L. M. Sander, P. Ramanlal, and E. Ben-Jacob, Phys. Rev. A **32**, 3160 (1985).

[10]T. A. Witten and L. M. Sander, Phys. Rev. B **27**, 5686 (1983).

[11]T. Vicsek, Phys. Rev. Lett. **53**, 2281 (1984).

[12]L. P. Kadanoff, J.Statist. Phys. **39**, 267 (1985).

[13]P. Garik, R. Richter, J. Hautman, and P. Ramanlal, Phys. Rev. A **32**, 3156 (1985).

[14]G. Daccord, J. Nittmann, and H. E. Stanley, Phys. Rev. Lett. **56**, 336 (1986).

[15]M. Matsushita, M. Sano, Y. Hayakawa, H. Honjo, and Y. Sawada, Phys. Rev. Lett. **53**, 286 (1984).

[16]R. M. Brady and R. C. Ball, Nature (London) **309**, 225 (1984).

[17]L. Paterson, J. Fluid Mech. **113**, 513 (1981), and Phys. Rev. Lett. **52**, 1621 (1984).

[18]L. Paterson, Phys. Fluids **28**, 26 (1985).

[19]W. W. Mullins and R. F. Sekerka, J. Appl. Phys. **34**, 323 (1963).

[20]E. Ben-Jacob, P. Garik, and T. M. Mueller, to be published.

[21]S. N. Rauseo, P. D. Barnes, and J. V. Maher, to be published.

[22]P. Tabeling and A. Libchaber, Phys. Rev. A **33**, 794 (1986).

[23]V. Steinberg, private communication.

[24]E. Ben-Jacob, P. Garik, and N. D. Goldenfeld, to be published.

(a)

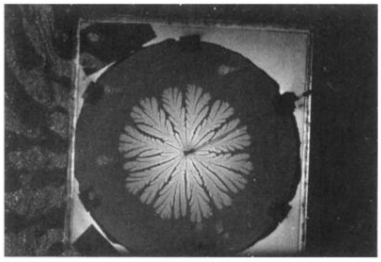

(b)

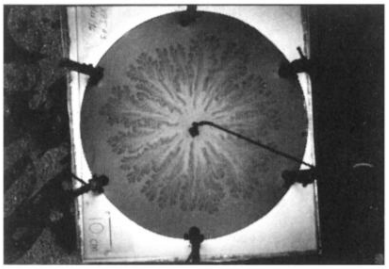

FIG. 1. The dense branching morphology generated in the Hele-Shaw cell described in the text. (a) Air into glycerol at applied pressure of 100 mm of Hg and spacing of ≈ 0.5 mm. (b) Water into glycerol at flow rate of 50 ml/min and spacing of ≈ 0.5 mm.

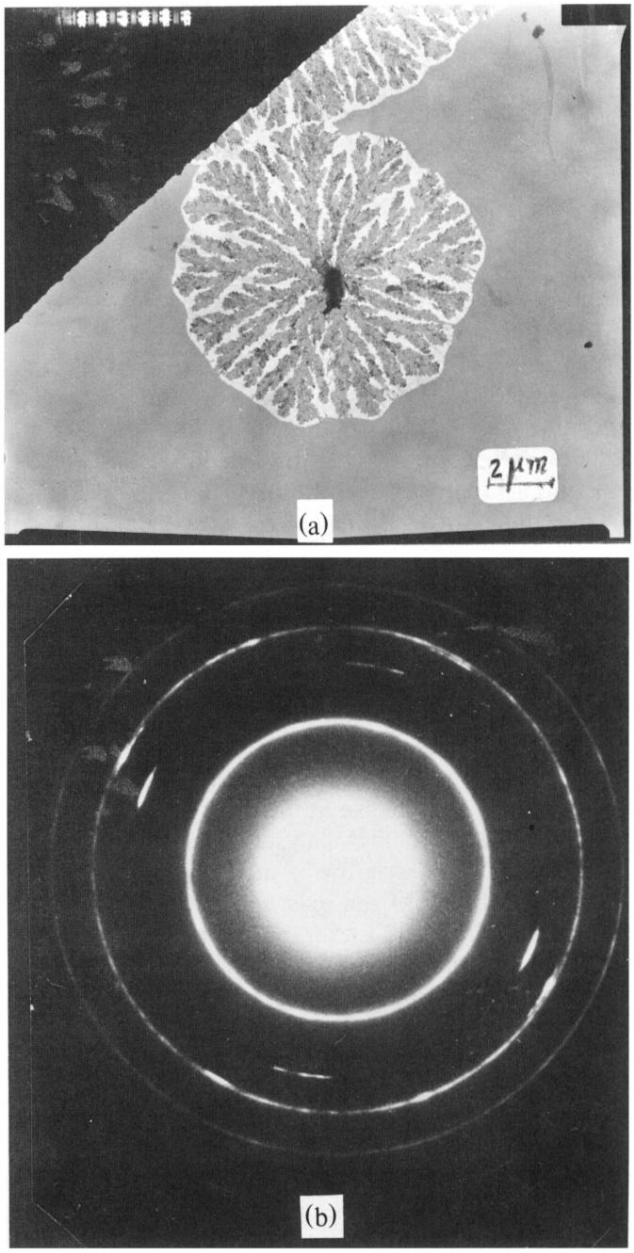

FIG. 3. (a) The DBM generated in the annealing of amorphous $Al_{0.4}Ge_{0.6}$. The dark structure is polycrystalline Ge. The light background is the crystalline Al matrix described in the text. The surrounding dark background is amorphous $Al_{0.4}Ge_{0.6}$. (b) Electron diffraction pattern from a dense branching morphology like that in (a). The bright arc spots are the (111) planes of Al. The rings are due to the diamond structure of polycrystalline Ge.